

SECONDARY RADIATION FROM THE PAMELA/ATIC EXCESS AND RELEVANCE FOR FERMI

E. BORRIELLO¹, A. CUOCO² AND G. MIELE¹

¹Dipartimento di Scienze Fisiche, Università di Napoli “Federico II” & INFN Sezione di Napoli,
 Complesso Universitario di Monte S. Angelo, Via Cinthia 80126, Napoli, Italy

²Department of Physics and Astronomy, University of Aarhus, Ny Munkegade, Bygn. 1520 8000, Aarhus, Denmark

Draft version May 18, 2009

ABSTRACT

The excess of electrons/positrons observed by the Pamela and ATIC experiments gives rise to a noticeable amount of synchrotron and Inverse Compton Scattering (ICS) radiation when the e^+e^- interact with the Galactic Magnetic Field, and the InterStellar Radiation Field (ISRF). In particular, the ICS signal produced within the WIMP annihilation interpretation of the Pamela/ATIC excess shows already some tension with the EGRET data. On the other hand, 1 yr of Fermi data taking will be enough to rule out or confirm this scenario with a high confidence level. The ICS radiation produces a peculiar and clean “ICS Haze” feature, as well, which can be used to discriminate between the astrophysical and Dark Matter scenarios. This ICS signature is very prominent even several degrees away from the galactic center, and it is thus a very robust prediction with respect to the choice of the DM profile and the uncertainties in the ISRF.

PACS: 95.35.+d, 95.85.Bh, 95.85.Pw, 98.70.Vc

Subject headings: dark matter — gamma rays: observations — cosmic rays — radio continuum: ISM — ISM: general — Galaxy: general

The Pamela and ATIC results have recently raised a great interest in the scientific community due to the possibility that the observed e^+e^- excesses could be a signature of the, so-far elusive, particle associated to Dark Matter. The raise in the positron fraction above 10 GeV until \sim 100 GeV seen by Pamela (Adriani et al. 2008a) and the excess of the sum of e^+ and e^- between \sim 100 GeV and \sim 700 GeV seen by ATIC (Chang et al. 2008) can be hardly explained in a standard Cosmic Ray production scenario and, instead, seem to point to a new source of e^+ and e^- . Hints of this anomaly were reported also by different experiments like HEAT (Barwick et al. 1997), AMS-01 (Aguilar et al. 2007; Alcaraz et al. 2000) and PPB-BETS (Torii et al. 2008). In addition, HESS has recently presented a measurement of the electron spectrum in the range $0.6 < E < 5$ TeV (Aharonian et al. 2008). This anomaly can have a standard astrophysical interpretation (Atoian et al. 1995, Zhang and Cheng 2001, Profumo 2008, Yuksel et al. 2008, Hooper et al. 2009) or an exotic one involving decaying (Liu et al. 2008, Hisano et al. 2008b, Yin et al. 2008, Chen et al. 2008, Ibarra and Tran, Hamaguchi et al. 2008) or the annihilation of DM particles (Hisano et al. 2008a, Mardon et al. 2009, Zurek 2008, Cholis et al. 2008a, Bergstrom et al. 2008a, Arkani-Hamed et al. 2009, Meade et al. 2009, Ishiwata et al. 2008a, Hu et al. 2009, Nomura and Thaler 2008, Hall and Hooper 2008, Barger et al. 2009, deBoer 2009, Cholis et al. 2008b, Fox and Poppitz 2008). The latter description, in particular, seems to favor a DM particle in the TeV range and with a thermally averaged annihilation cross section $\langle\sigma_A v\rangle \sim 10^{-23} \text{ cm}^3 \text{s}^{-1}$. However, this scenario faces several difficulties. A first problem is that, differently from the positron ratio, no excess is observed by Pamela in the antiproton over proton ratio (Adriani et al. 2008b).

This means that DM decay/annihilation into hadronic channels is mainly forbidden or at least strongly suppressed (Cirelli et al. 2008; Donato et al. 2008), and hence one has to resort to models in which only the leptonic channels are allowed. The second problem is that the annihilation rate required to explain the anomaly is about three orders of magnitude above the natural expectation of $\langle\sigma_A v\rangle \sim 3 \times 10^{-26} \text{ cm}^3 \text{s}^{-1}$ for a DM thermal relic which accounts for the cosmological DM abundance. This requires either the introduction of large annihilation boost factors from the presence of galactic substructure, or some enhancing annihilation mechanism like the Sommerfeld process (Lattanzi and Silk 2008; Ibe et al. 2008).

The fact that hadronic channels have to be suppressed to explain the Pamela/ATIC anomaly implies that only few (energetic) photons are produced either if the annihilation takes place through the $\mu^+\mu^-$ or $\tau^+\tau^-$ channels or in the case of the e^+e^- channel through the presence of Final State Radiation. With the limited contribution of gamma rays accompanying the annihilation process, the constraints from gamma observations become thus quite weak. Anyway, even though only e^+e^- were produced in the DM annihilation process, these leptons, once in the galactic environment, would interact with the Galactic Magnetic Field (GMF) and the Interstellar Radiation Field (ISRF). Thus they would lose energy producing synchrotron radiation in the radio band and Inverse Compton Scattering (ICS) Radiation in the gamma band. This secondary radiation thus represents a complementary observable to constrain the DM signal (Bergstrom et al. 2008b, Ishiwata et al. 2008b, Cholis et al. 2008c, Nardi et al. 2008, Zhang et al. 2008, Bertone et al. 2008, Borriello et al. 2008). In the following we will focus on the synchrotron and ICS signals which are expected in the galactic halo. With

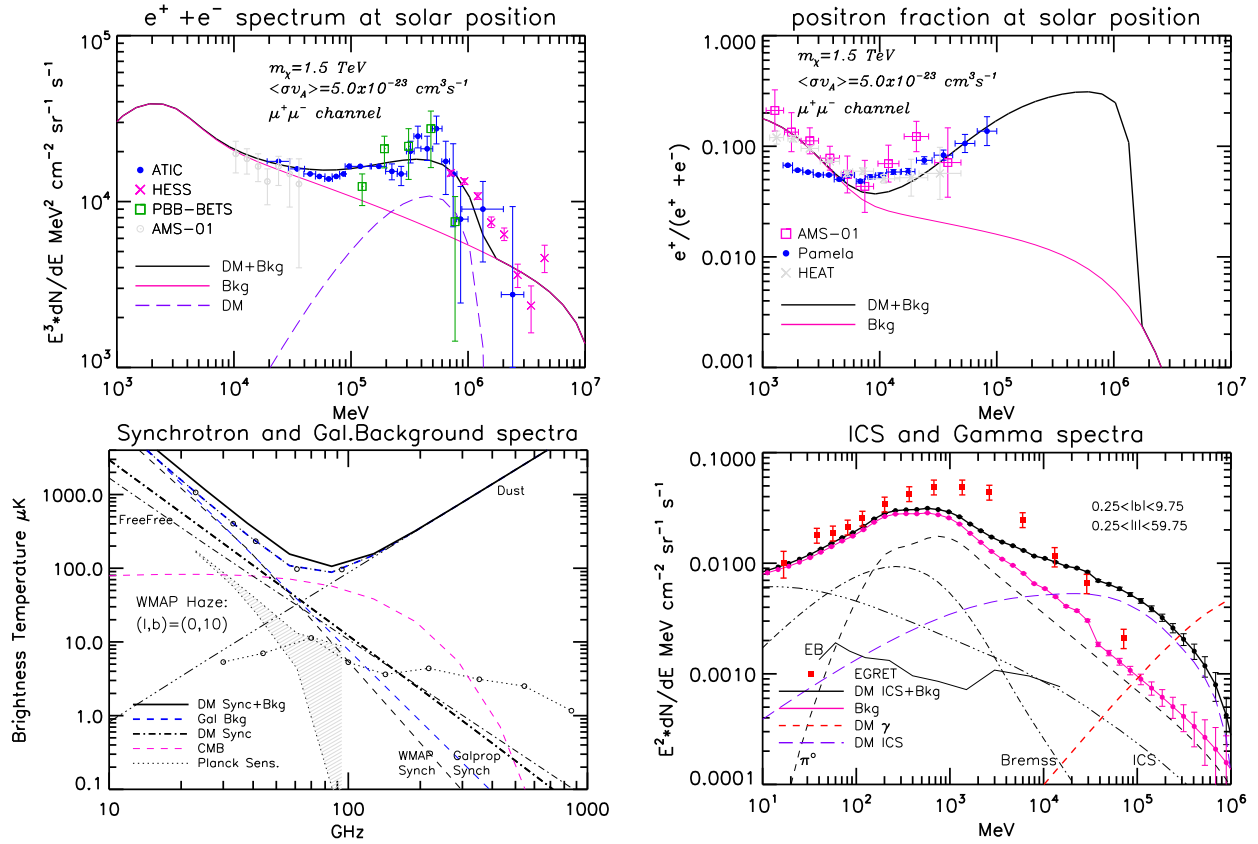


FIG. 1.— The upper panels show the positron fraction and the total e^+e^- spectrum for the CR background and the DM annihilation signal compared with the Pamela and ATIC data. A compilation of previous data (HEAT (Barwick et al. 1997) and AMS-01 (Aguilar et al. 2007) for the positron fraction and PPB-BETS (Torii et al. 2008), AMS-01 (Alcaraz et al. 2000) and HESS (Aharonian et al. 2008) for the e^+e^- spectrum) is also shown. The lower right panel reports the gamma spectrum for the CR background and the ICS signal from DM electrons in the Halo together with the EGRET measurements and the errors expected after a 1 yr survey at Fermi. The red dashed curve shows the spectrum of gamma-rays produced directly through the annihilation into $\mu^+\mu^-$. The decomposition of the CR background into the IC, bremsstrahlung, pion decay and extragalactic components is reported as well. The lower left panel shows the DM synchrotron emission, in units of brightness temperature, 10° away from the GC compared with the galactic backgrounds as measured by WMAP (Gold et al. 2008) and the r.m.s. fluctuations of the CMB. The open points indicate the 9 Planck frequencies while the dotted line shows the expected Planck sensitivity for a 14 months survey (Planck Collaboration 2006). The second set of open points indicates the WMAP frequencies. For comparison it is shown the signal from the WMAP Haze 10° degrees away from the GC as derived in (Dobler and Finkbeiner 2007). Furthermore we report the decomposition of the Galactic backgrounds into the dust, free-free and synchrotron components together with the synchrotron background derived with Galprop. A model with a WIMP of $m_\chi = 1.5$ TeV which annihilates only into $\mu^+\mu^-$ with a rate $\langle\sigma_A v\rangle \sim 5 \times 10^{-23} \text{ cm}^3 \text{ s}^{-1}$ is considered for all the plots. The propagation parameters are specified in the text.

respect to focussing on the Galactic Center (GC) this approach provides much more robust predictions due to the weaker dependence on the choice of the DM profile and thanks to the smaller uncertainties on ISRF and GMF. The relevance of ICS signal in relation to Pamela has been, indeed, discussed in recent papers (Zhang et al. 2008; Cholis et al. 2008c) which show the presence of some tension with the EGRET data as well. In the following, we will stress how the situation is expected to change with the new data from Fermi and, further, we will investigate the peculiar spatial distribution which the DM signal is expected to produce.

We use for the calculations a slightly modified version of Galprop v50.1p (Strong and Moskalenko 1998; Moskalenko and Strong 1997), which solves numerically the electron diffusion-loss equation and produces the ICS and synchrotron maps. The code also provides maps of the CR gamma diffuse emission using available data on the CR abundances and the distribution of galactic gas. For our calculations we employ a diffusion coefficient $D = D_0(E/E_0)^{-\alpha}$ with $D_0 = 5 \times 10^{28} \text{ cm}^2 \text{ s}^{-1}$, $E_0 = 3 \text{ GeV}$ and $\alpha = 0.33$, corresponding to a Kolmogorov spectrum of turbulence. The transport equation is solved in a cylinder of half-height $z = \pm 4 \text{ kpc}$

and radius $R = 20 \text{ kpc}$, while the GMF used to derive the synchrotron radiation is modeled as $\langle B^2 \rangle^{1/2} = B_0 \exp(-r/r_B - |z|/z_B)$ with $B_0 = 11 \mu\text{G}$ $r_B = 10 \text{ kpc}$ and $z_B = 2 \text{ kpc}$. It is worth reminding, however, that electrons have typically a quite short propagation length (in terms of the galactic size) corresponding to a path of $\mathcal{O}(1 \text{ kpc})$ (Delahaye et al. 2007) before losing a significant percentage of their energy. Thus the final spectrum and distribution of electrons keep only a weak dependence on the chosen propagation parameters. The GMF, on the other hand, is still affected by large uncertainties especially in the inner kpc's of the galaxy (see (Han 2009) and reference therein for a recent review). The synchrotron radiation, which is quite dependent on the GMF, shares, thus, a similar uncertainty on the normalization. The InterStellar Radiation Field, which is the photon target that determines the ICS signal, is, instead, better known and the derived ICS signal is thus a more robust prediction than the synchrotron signal. The ISRF implemented in Galprop is described in details in (Porter and Strong 2005). Finally, for the DM profile we choose a very conservative isothermal cored one, namely $\rho(r) = \rho_0 (r_c^2 + r_\odot^2) / (r_c^2 + r^2)$, with a DM

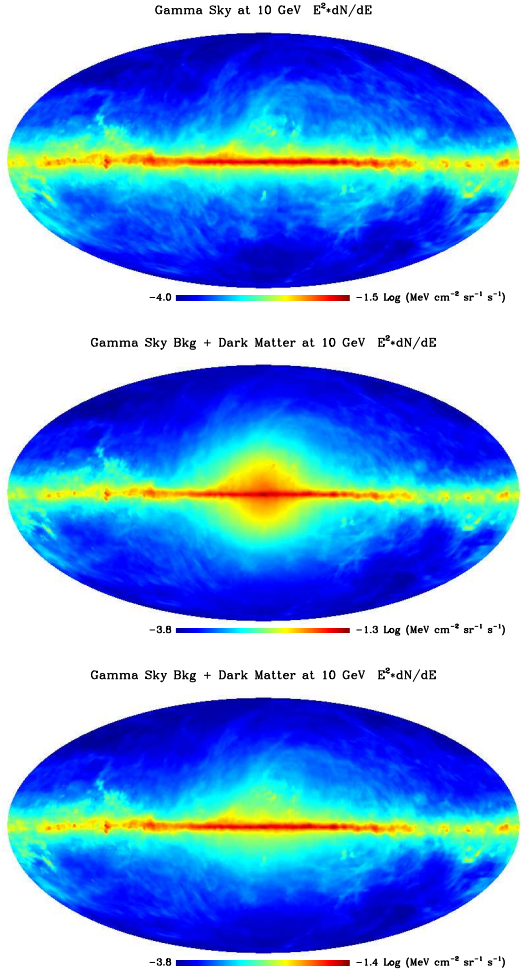


FIG. 2.— Sky map (in healpix format (Gorski et al. 2004)) of galactic gamma backgrounds at the energy of 10 GeV (top). The same with the inclusion of the DM annihilation contribution (center) or Decaying DM (bottom).

density $\rho_0 = 0.4 \text{ GeV/cm}^3$ at the solar position $r_\odot = 8.5 \text{ kpc}$. We fix $r_c = 2.8 \text{ kpc}$ for the the core size. However, this particular choice is not crucial since we are going to calculate the signal not in GC, but the one coming from the Halo where the uncertainties on the details of DM profile are less relevant.

We choose to study a single benchmark model with a WIMP of $m_\chi = 1.5 \text{ TeV}$ annihilating in the $\mu^+ \mu^-$ channel only with a rate $\langle \sigma_A v \rangle \sim 5 \times 10^{-23} \text{ cm}^3 \text{s}^{-1}$. The resulting electron/positron injection spectrum dN_e/dE has approximately a constant behavior in energy with a cutoff at the mass of the WIMP. We calculate dN_e/dE with DarkSUSY (Gondolo et al. 2004), which, in turn, uses a tabulation of the spectrum of the decay products derived with Pythia (Sjostrand 2007). The electron source term for Galprop is then given by $Q(r, E) = \rho^2 \langle \sigma_A v \rangle / 2m_\chi^2 \times dN_e/dE$. This model provides a reasonable good match with the Pamela and ATIC data. It is certainly possible to achieve a better fit with a mixing of the various leptonic channels, or with particular alternative annihilation mechanism or, further, with a fine tuning of the propagation parameters¹. How-

¹ During the review procedure of our paper the Fermi collaboration has reported a measurement of the $e^+ e^-$ flux in the same

ever, since the aim of our paper is to focus on the secondary radiation, the final results would be only weakly affected by the above details on the WIMPs annihilation process. The results are illustrated in Fig.1. The upper panels show the comparison of the model with the Pamela and ATIC data and with a compilation of previous data showing that, indeed, the agreement is good. The secondary radiation results are shown in the lower panels. The right one shows the expected difference between the CR gamma background and the ICS produced by the population of DM electrons distributed in the galactic halo together with the EGRET measurements (as taken from (Strong et al. 2004b)). Furthermore the decomposition of the CR background into the IC, bremsstrahlung, pion decay and extragalactic components is also shown. The extragalactic component (Sreekumar et al. 1998) is from the reanalysis of the EGRET data from (Strong et al. 2004a). The small error bars are a forecast for $T=1 \text{ yr}$ of data taking by Fermi assuming the effective area as function of energy as taken from (Atwood et al. 2009) (roughly $A_{eff} = 8000 \text{ cm}^2$ above $\sim 1 \text{ GeV}$) a field of view of 2.4 sr and no CR contamination hence $N_\gamma = T \times \text{fov} \times f_\Delta \times \int_{\Delta E} A_{eff}(E) dN_\gamma/dE(E) dE$. $dN_\gamma/dE(E)$ is the gamma ray flux while f_Δ is the fraction of area of the sky where the signal is integrated. The Poisson error is then $\propto 1/\sqrt{N_\gamma}$. Finally the errors are shown for a logarithmic binning of the energy.

It is worth noticing that the errors expected for one year from Fermi survey are tiny enough to detect the excess with an high degree of confidence. Even more importantly, this excess comes from the halo region, placed several degrees away from the GC and thus in a region were the uncertainties on the DM profile are expected to be much smaller. Also the uncertainty on the ISRF, which seems anyway not critical (Porter and Strong 2005), naturally decreases moving away from the GC. A possible problem is, in principle, the fact that the DM excess can be mistaken with a not well understood CR gamma background. Indeed, the situation is similar to the EGRET GeV excess (Hunter et al. 1997) which, in principle can be explained either with an “optimized” CR model (Strong et al. 2004b) or with a DM contribution (deBoer et al. 2005)². In this case, however, the IC excess produced by Pamela/ATIC is more properly a “10-100 GeV excess”. Moreover, it generally exceeds already the EGRET data, although by an amount which is still in principle within the EGRET systematics. A more crucial difference is however the spatial distribution. While the GeV excess is almost isotropic in the sky, the ICS excess has the shape of a circular Haze reflecting the DM distribution in the Halo. This difference, indeed, is quite striking, as can be seen clearly in Fig.2.

energy range of ATIC (Abdo et al. 2009). The spectrum measured by Fermi confirms an excess with respect to the conventional cosmic ray model although the excess is less prominent and smoother than the one reported by ATIC. For this broad smooth excess a better fit can be achieved through an annihilation into $\tau^+ \tau^-$ instead of $\mu^+ \mu^-$. Using the $\tau^+ \tau^-$ channel as benchmark model, however, produces just minor changes in the results derived in the following.

² Note, anyway, that preliminary results from the Fermi collaboration seem not to confirm the GeV excess. See e.g. the talk presented on behalf of the Fermi collaboration at the January 2009 meeting of the AAS.

The CR background instead is expected to lie mostly along the galactic plane where the astrophysical sources are located.

The lower left panel shows the DM synchrotron emission in units of brightness temperature ($T \propto \nu^{-2} F_\nu$) 10° away from the GC compared with the galactic backgrounds. We use the WMAP background maps (CMB subtracted) and their decomposition into synchrotron, free-free and dust (Gold et al. 2008)³. For illustration the frequency spectra in the plot are extrapolated also outside the WMAP frequency coverage. We also show for comparison the background synchrotron emission calculated with Galprop which, indeed, exhibits a close match with the WMAP synchrotron spectrum in the 20-100 GHz range. It has to be noticed that the synchrotron galactic CR emission dominates the background only up to a frequency of ~ 60 GHz, then there is a small frequency window which is dominated by free-free (thermal bremsstrahlung) emission, while above ~ 100 GHz the background is dominated by dust emission. The fluctuations of the CMB dominates around ~ 100 GHz depending on the galactic latitude. The high quality data from WMAP, however, allow to efficiently clean this further “background”. The DM synchrotron radiation would exhibit in principle a peak with respect to the synchrotron background around a frequency $\sim 10^5$ GHz (as shown in (Zhang et al. 2008)), where, however, the dust background is dominating by many orders of magnitude. Restricting the analysis in the more interesting frequency range < 1000 GHz, the DM signal has an almost power law behavior with a slope slightly harder than the background, while the spatial distribution has a circular shape. These characteristics indeed correspond to what is found in the WMAP Haze (Dobler and Finkbeiner 2007; Hooper et al. 2007; Cumberbatch et al. 2009) whose signal we also report in the plot for comparison. Notice, however, that the Haze feature has still to be firmly established and that at the moment it is very much dependent on the method employed to separate the foregrounds (Gold et al. 2008). Interestingly, we find that, for the GMF model employed, the DM signal exceeds the Haze for a factor of ~ 3 similarly to the IC case. The theoretical signal, on the other hand is affected by the uncertainties on the GMF and it is difficult to normalize reliably. Moreover, further uncertainties come from the systematics involved in the separations of the measured signal into the various components, synchrotron, dust, free-free and DM, hence it would be difficult to asses the real significance of this excess.

We also consider the case of electrons arising from WIMP decay considering a DM signal following linearly the halo profile and with the same electron injection spectrum as for the $\mu^+ \mu^-$ channel. Formally, at the solar position, up to diffusion effects, exactly the same positron fraction and electron spectrum can be obtained setting the DM decay rate to $\Gamma = \rho_0 \langle \sigma_A v \rangle / 2m_\chi$. The ICS radiation from the Halo is however significantly reduced although Fermi can still discriminate this possibility as shown in Fig.2 and Fig.3. At this level, however, the confusion with a not well understood background could

³ Data are available at the Lambda web site: <http://lambda.gsfc.nasa.gov/>

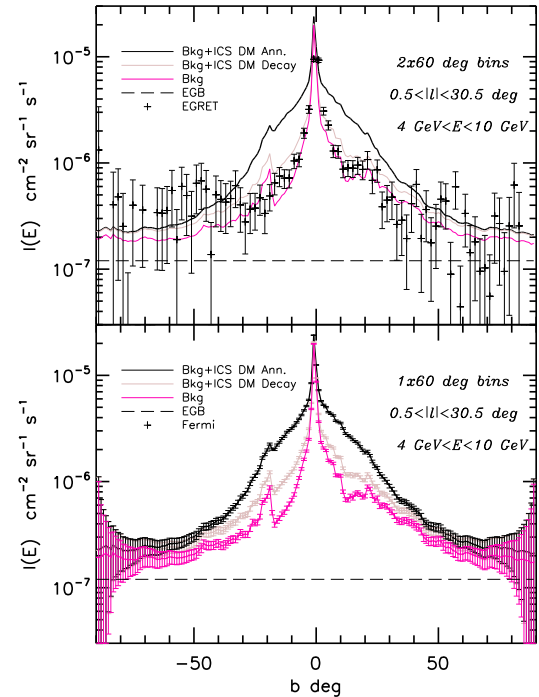


FIG. 3.— Top panel: Background and DM (either annihilating and decaying) latitude gamma profiles averaged in a strip of 60° along $l = 0$ compared with the EGRET data. Bottom panel: same as above, but with the errors expected with a 1yr survey from Fermi. At high latitudes the error bars appear artificially to increase for the geometry of the $0.5^\circ < |l| < 30.5^\circ$ strip (which is effectively shrinking along b).

become more problematic although the peculiar circular shape of the ICS Haze, present also in this case (see Fig.2), can help to distinguish the DM signal from the astrophysical background.

Finally, in Fig.3 we report another forecast example of the excellent Fermi ability to discriminate among the astrophysical and annihilating DM scenario considering the latitude profile and a strip of 60° width along $l = 0$. We also show in the upper panel the EGRET data in the same region and energy range (as derived with the Galplot package (see also (Strong et al. 2004b))). Compared with the EGRET data the annihilation model seems to produce a too much broad peak to fit the data, beside producing an excessively high normalization. The decaying model is instead difficult to separate from the background within the EGRET error bars. With the upcoming Fermi data at hands, the analysis can be easily generalized to exploit the full angular shape of the IC Haze. This would clearly offer the optimal sensitivity to disentangle the different scenarios.

In summary, we have shown that Fermi has the potential to test the DM interpretation of Pamela/ATIC basically in a model independent way thanks to the strong IC signal which the Pamela/ATIC electrons would themselves produce in the galactic halo. The EGRET data seems, indeed, already to disfavor the DM annihilation interpretation. Further, the IC signal give rise to a striking “IC Haze” feature peaking around 10-100 GeV which would provide a further mean to discriminate the DM signal from the astrophysical backgrounds and/or to check for possible systematics.

Acknowledgements: G. Miele acknowledge supports by INFN - I.S. FA51 and by PRIN 2006 “Fisica Astroparticellare: Neutrini ed Universo Primordiale” of Italian MIUR.

REFERENCES

Abdo A. *et al.* [Fermi Collaboration], Phys. Rev. Lett. **102** (2009) 181101 [arXiv:0905.0025 [astro-ph.HE]].

Adriani O. *et al.* [PAMELA Collaboration], 2008, arXiv:0810.4995.

Adriani O. *et al.*, Phys. Rev. Lett. **102** (2009) 051101

Aguilar M. *et al.* [AMS-01 Collaboration], Phys. Lett. B **646**, 145 (2007) [arXiv:astro-ph/0703154].

Aharonian F. *et al.* [H.E.S.S. Collaboration], Phys. Rev. Lett. **101**, 261104 (2008) [arXiv:0811.3894].

Alcaraz J. *et al.* [AMS Collaboration], Phys. Lett. B **484**, 10 (2000) [Erratum-ibid. B **495**, 440 (2000)].

Arkani-Hamed N., Finkbeiner D.P., Slatyer T. and Weiner N., Phys. Rev. D **79** (2009) 015014 [arXiv:0810.0713].

Atoian A.M., Aharonian F.A. and Volk H.G., Phys. Rev. D **52**, 3265 (1995). Aharonian F.A., Atoian A.M. and Volk H.J., A&A **294**, L41 (1995).

Atwood F.W.B. *et al.* [LAT Collaboration], 2009, arXiv:0902.1089.

V. Barger *et al.*, Phys. Lett. B **672**, 141 (2009) [arXiv:0809.0162].

Barwick S.W. *et al.* [HEAT Collaboration], Astrophys. J. **482**, L191 (1997) [arXiv:astro-ph/9703192].

Bergstrom L., Bringmann T. and Edsjo J., Phys. Rev. D **78**, 103520 (2008a) [arXiv:0808.3725].

Bergstrom L., Bertone G., Bringmann T., Edsjo J. and Taoso M., 2008b, arXiv:0812.3895

Bertone G., Cirelli M., Strumia A. and Taoso M., 2008, arXiv:0811.3744.

Borriello E., Cuoco A. and Miele G., Phys. Rev. D **79** (2009) 023518

Chang J. *et al.*, Nature **456**, 362 (2008).

Chen C.R., Takahashi F. and Yanagida T.T., 2008, arXiv:0811.0477. Chen C.R. *et al.*, 2008, arXiv:0811.3357.

Cholis I., Goodenough L., Hooper D., Simet M. and Weiner N., 2008a, arXiv:0809.1683.

Cholis I. *et al.*, 2008b, arXiv:0810.5344.

Cholis I., Dobler G., Finkbeiner D.P., Goodenough L. and Weiner N., 2008b, arXiv:0811.3641.

Cirelli M., Kadastik M., Raidal M. and Strumia A., 2008, arXiv:0809.2409. Cirelli M. and Strumia A., 2008, arXiv:0808.3867.

Cumberbatch D.T. *et al.*, 2009, arXiv:0902.0039.

deBoer W., Sander C., Zhukov V., Gladyshev A.V. and Kazakov D.I., Astron. Astrophys. **444** (2005) 51

deBoer W., 2009, arXiv:0901.2941.

Delahaye T., Lineros R., Donato F., Fornengo N. and Salati P., Phys. Rev. D **77**, 063527 (2008).

Dobler G. and Finkbeiner D.P., 2007, arXiv:0712.1038.

Donato F., Maurin D., Brun P., Delahaye T. and Salati P., Phys. Rev. Lett. **102** (2009) 071301 [arXiv:0810.5292].

Fox P.J. and Poppitz E., 2008, arXiv:0811.0399.

Gold B. *et al.* [WMAP Collaboration], Astrophys. J. Suppl. **180** (2009) 265, arXiv:0803.0715.

Gondolo P., Edsjo J., Ullio P., Bergstrom L., Schelke M. and Baltz E.A., JCAP **0407** (2004) 008 [astro-ph/0406204].

Gorski K. M. *et al.*, Astrophys. J. **622** (2005) 759

Hall J. and Hooper D., 2008, arXiv:0811.3362.

Hamaguchi K. *et al.*, 2008, arXiv:0811.0737.

Han J.L., 2009, arXiv:0901.1165.

Hisano J., Kawasaki M., Kohri K. and Nakayama K., 2008a arXiv:0810.1892.

Hisano J., Kawasaki M., Kohri K. and Nakayama K., 2008b arXiv:0812.0219. J. Hisano *et al.*, 2009 arXiv:0901.3582.

Hooper D., Finkbeiner D.P. and Dobler G., Phys. Rev. D **76** (2007) 083012 [arXiv:0705.3655].

Hooper D., Blasi P. and Serpico P.D., JCAP **0901**, 025 (2009)

Hu H.B. *et al.*, 2009, arXiv:0901.1520 [astro-ph].

Hunter S.D. *et al.*, Astrophys. J. **481** (1997) 205.

Ibarra A. and Tran D., 2008, arXiv:0811.1555.

Ibe M., Murayama H. and Yanagida T.T., 2008 arXiv:0812.0072.

Ishiwata K., Matsumoto S. and Moroi T., 2008a, arXiv:0811.0250.

Ishiwata K., Matsumoto S. and Moroi T., 2008b, arXiv:0811.4492.

Lattanzi M. and Silk J.I., 2008, arXiv:0812.0360.

Liu J., Yin P.f. and Zhu S.h., 2008, arXiv:0812.0964.

Mardon J., Nomura Y., Stolarski D. and Thaler J., 2009, arXiv:0901.2926.

Meade P., Papucci M. and Volansky T., 2009, arXiv:0901.2925.

Moskalenko I.W. and Strong A.W., Astrophys. J. **493** (1998) 694

Nardi E., Sannino F. and Strumia A., JCAP **0901** (2009) 043

Nomura Y. and Thaler J., 2008, arXiv:0810.5397.

Planck Collaboration, “Planck: The scientific programme,” 2006, astro-ph/0604069.

Porter T.A. and Strong A.W., 2005, arXiv:astro-ph/0507119.

Profumo S., 2008, arXiv:0812.4457.

Sjostrand T., Mrenna S. and Skands P., Comput. Phys. Commun. **178** (2008) 852 [arXiv:0710.3820].

Sreekumar P. *et al.* [EGRET Collaboration], Astrophys. J. **494** (1998) 523 [astro-ph/9709257].

Strong A.W. and Moskalenko I.W., Astrophys. J. **509** (1998) 212

Strong A.W., Moskalenko I.W. and Reimer O., Astrophys. J. **613** (2004a) 956 [astro-ph/0405441].

Strong A.W., Moskalenko I.W. and Reimer O., Astrophys. J. **613** (2004b) 962 [astro-ph/0406254].

Torii S. *et al.* [PPB-BETS Collaboration], 2008 arXiv:0809.0760.

Yin P.f., Yuan Q., Liu J., Zhang J., Bi X.j. and Zhu S.h., Phys. Rev. D **79**, 023512 (2009) [arXiv:0811.0176].

Yuksel H., Kistler M.D. and Stanev T., 2008, arXiv:0810.2784 [astro-ph].

Zhang L. and Cheng K.S. A&A **368**, 1063(2001).

Zhang J., Bi X.j., Liu J., Liu S.M., Yin P.f., Yuan Q. and Zhu S.h., 2008 arXiv:0812.0522.

Zurek K.M., 2008, arXiv:0811.4429.